

Published in final edited form as:

Neuron. 2008 November 26; 60(4): 570–581. doi:10.1016/j.neuron.2008.08.022.

The brain in chronic CRPS pain: Abnormal gray-white matter interactions in emotional and autonomic regions

Paul Y. Geha¹, Marwan N. Baliki¹, R. Norman Harden², William R. Bauer³, Todd B. Parrish⁴, and A. Vania Apkarian^{1,5,6,*}

¹Department of Physiology, Northwestern University, Feinberg School of Medicine, Chicago IL 60611

²Rehabilitation Institute, Northwestern University, Feinberg School of Medicine, Chicago IL 60611

³Department of Neuroscience, University of Toledo, 3000 Arlington Ave., Toledo OH 43614-2598

⁴Department of Radiology, Northwestern University, Feinberg School of Medicine, Chicago IL 60611

⁵Department of Anesthesia, Northwestern University, Feinberg School of Medicine, Chicago IL 60611

⁶Department of Surgery, Northwestern University, Feinberg School of Medicine, Chicago IL 60611

Summary

Chronic complex regional pain syndrome (CRPS) is a debilitating pain condition accompanied by autonomic abnormalities. We investigated gray matter morphometry and white matter anisotropy in CRPS patients and matched controls. Patients exhibited 1) a disrupted relationship between white matter anisotropy and whole-brain gray matter volume, 2) gray matter atrophy in a single cluster encompassing right insula, right ventromedial prefrontal cortex (VMPFC), and right nucleus accumbens, and 3) a decrease in fractional anisotropy in the left cingulum-callosal bundle. Reorganization of white matter connectivity in these regions was characterized by branching pattern alterations, and increased (VMPFC to insula) and decreased connectivity (VMPFC to basal ganglion). While regional atrophy differentially related to pain intensity and duration, the strength of connectivity between specific atrophied regions related to anxiety. These abnormalities encompass emotional, autonomic, and pain perception regions, implying that they likely play a critical role in the global clinical picture of CRPS.

Keywords

DTI; VBM; insula; chronic pain; RSD; prefrontal cortex

Introduction

Complex regional pain syndrome (CRPS) is an inflammatory and/or neuropathic condition that develops after trauma, most commonly seen following injury to the limbs (Harden et al., 2007; Janig and Baron, 2003). The condition is characterized by various exaggerated painful sensations (spontaneous and/or evoked), abnormal regulation of blood flow in the affected region, as well as sweating, edema, trophic changes of skin and subcutaneous tissues, and motor

*Corresponding author: A. Vania Apkarian, a-apkarian@northwestern.edu.

Publisher's Disclaimer: This is a PDF file of an unedited manuscript that has been accepted for publication. As a service to our customers we are providing this early version of the manuscript. The manuscript will undergo copyediting, typesetting, and review of the resulting proof before it is published in its final citable form. Please note that during the production process errors may be discovered which could affect the content, and all legal disclaimers that apply to the journal pertain.

disorders. CRPS develops idiopathically in less than 5% of limb traumas (Birklein et al., 2001; Stanton-Hicks et al., 1995; Veldman et al., 1993). Once the condition becomes chronic (> 3 months after healing of injury) it is usually highly debilitating with patients experiencing long-term suffering. Underlying mechanisms are poorly characterized, and some clinical scientists have questioned whether the condition is a single coherent entity (Ochoa, 1992). As efforts to identify specific peripheral mechanisms for the condition have been unsuccessful research has shifted to central mechanisms (Harden et al., 2001; Janig and Baron, 2002; Janig and Baron, 2003). Functional brain imaging studies indicate that such patients exhibit abnormal or shifted brain activity to motor tasks, imagined motor tasks, and to tactile stimuli, and also show that the extent of observed functional reorganizations are linked to properties of CRPS pain (Gieteling et al., 2008; Maihofner et al., 2003; Maihofner et al., 2007; Pleger et al., 2006). Other studies show that CRPS pain engages many regions commonly seen for acute pain as well as prefrontal cortical regions (Apkarian et al., 2001; Maihofner et al., 2005; Maihofner et al., 2006). CRPS patients have lower perceptual learning aptitude (Maihofner and DeCol, 2007), and exhibit blunted emotional decision-making abilities (Apkarian et al., 2004a).

Here we study the morphology of the brain in CRPS patients using automated voxel based morphometry (VBM), try to inter-relate changes in gray matter to reorganization of the connectivity of the white matter, using diffusion tensor imaging (DTI) analyses, and link these brain derived parameters to the clinical characteristics of CRPS. Recent morphometry studies show that in diverse chronic pain conditions the human brain exhibits specific gray matter abnormalities (primarily regional atrophy), preferentially impacting the lateral or medial prefrontal cortex depending on the condition (Apkarian et al., 2004b; Kuchinad et al., 2007; Schmidt-Wilcke et al., 2005; Schmidt-Wilcke et al., 2006; Valfre et al., 2008). Thus if chronic CRPS has a prominent central component then it should exhibit unique brain morphological abnormalities. The performance of CRPS patients on an emotional decision-making task is far worse than in chronic back pain patients, and matches the impairment seen in patients with ventromedial prefrontal (VMPFC) lesions (Apkarian et al., 2004a; Bechara et al., 1994). Therefore, we hypothesize that CRPS is characterized by gray matter atrophy in the VMPFC. Furthermore, since CRPS is the primary chronic pain condition commonly accompanied by autonomic abnormalities, cortical regions modulating autonomic outflow should also exhibit morphological abnormalities, which would again implicate the VMPFC as well as the anterior portion of the insula (AI), and dorsal anterior cingulate (ACC) (Critchley, 2005).

Recent advances in diffusion tensor magnetic resonance imaging (DTI) coupled with DTI derived probabilistic tractography take advantage of water diffusion along axons and allow the study of the integrity and structural connectivity of the white matter (Alexander et al., 2007; Beaulieu, 2002). Parameters derived from this local water diffusion can then be used to study white matter structure. By fitting a diffusion tensor model to DTI measurements at each voxel, one can measure fractional anisotropy (FA) and its three principle diffusivities (eigenvalues λ_1 , λ_2 , and λ_3), all of which characterize the microenvironment of the white matter tissue (Beaulieu, 2002). Additionally, using probabilistic tractography as derived from DTI (Behrens et al., 2003), one can study the connectivity for brain gray matter regions showing abnormalities in density or white matter anisotropy, and link local abnormalities in gray matter or in myelination to brain connectivity. Here we further develop new methods for quantifying connectivity and branching of that connectivity. To date there is no information regarding white matter properties in chronic pain.

Results

Whole-brain gray matter volume and white matter diffusion are inter-related and abnormal in CRPS

There was no difference in neocortical gray matter volume between CRPS patients and age and sex matched control subjects; there was also no difference in the size of the lateral ventricles between the two groups (Figure S1). Whole-brain neocortical gray matter volume correlated with age in both groups (CRPS subjects, age dependence slope = $-3.2 \text{ cm}^3/\text{year}$, $R^2 = 0.55$, $p < 10^{-4}$; healthy subjects, slope = $-1.9 \text{ cm}^3/\text{year}$, $R^2 = 0.22$, $p < 0.05$; these correlations were also significant when tested non-parametrically using Spearman Rank R, which compensates for the potential influence of outliers), with a trend for stronger correlation in CRPS ($p=0.09$) (Figure 1A). This age associated decrease in cortical gray matter volume matches previous estimates (Apkarian et al., 2004b; Good et al., 2001; Resnick et al., 2003).

Whole-brain skeletal FA (mean FA calculated over individual subjects' white matter skeleton), a global measure of water diffusion over white matter tracks that reflects integrity of the white matter (Alexander et al., 2007), as well as parallel and perpendicular diffusivities, did not differ between CRPS and matched control subjects, and corresponds to recent reports (Figure S2) (Giorgio et al., 2007; Kochunov et al., 2007). Because a primary objective of the present study was to inter-relate gray and white matter properties, we first examined such relationships over the whole-brain. Whole-brain skeletal FA showed a significant positive correlation with whole-brain gray matter volume in the healthy subjects ($R^2 = 0.58$, $p < 0.00003$; also significant non-parametrically) but not in the CRPS ($R^2 = 0.02$, $p > 0.60$; the slopes of the two fits were significantly different, $p < 0.008$) (Figure 1B, Figure S2). Age did not influence the relationship between whole-brain FA and whole-brain gray matter, in either group (multiple regression with age as covariate did not change the outcomes). This is a new finding with no previous estimates in the literature; it can be interpreted as evidence for a general disruption of the gray-white matter structural relationship in the CRPS compared to the healthy subjects.

Regional gray matter atrophy in the right medial prefrontal cortex and anterior insula in CRPS

Regional gray matter changes were assessed non-parametrically, using optimized VBM. A single cluster encompassing the right AI, orbital portion of VMPFC and extending posteriorly into nucleus accumbens (NAc) exhibited decreased gray matter density (cluster p -value = 0.05, corrected for multiple comparisons; cluster size = 3 cm^3 ; when a 9.2 mm smoothing kernel was used, Figure S3) in CRPS patients relative to matched healthy subjects (Figure 2A). The peak atrophy was located in AI [MNI x,y,z, coordinates (in millimeters) 28, 22, -10; t -value = 4.88, $p = 0.013$]. The possibility that this difference in gray matter density may be due to registration artifacts was ruled out (Figure S4A). Gray matter density values, extracted from the whole cluster, were significantly different between the groups ($p < 10^{-5}$), and showed a negative correlation with pain duration in CRPS ($R^2 = 0.33$, $p < 0.01$; also significant non-parametrically) (Figure 2A). Multiple regression of gray matter density to pain duration using age and gender as covariates indicated that pain duration was the only significant factor ($p < 0.006$), and showed that pain duration effect is four times larger than aging effect within this cluster. When the cluster was sub-divided into the underlying anatomical regions we found a significant negative correlation between gray matter density in the right VMPFC and the interaction between pain duration and pain intensity ($R^2 = 0.26$ $p < 0.05$; also significant non-parametrically) (Figure 2B); and a negative correlation between right AI gray matter density and pain duration ($R^2 = 0.33$ $p < 0.01$; only borderline significant non-parametrically) (Figure 2C). Because the CRPS patient population included patients suffering from CRPS pain localized to right, left, and bilateral body regions, we also studied the effect of sidedness by performing the VBM analysis separately for the unilateral CRPS groupings and respective

matched controls. The results showed that the same right AI and VMPFC region exhibited decrease in gray matter density regardless of sidedness (Figure S5).

Given that our population covered a wide age range and whole-brain gray matter volume suggested age related differences between the two groups, we investigated the pattern of gray matter density change in the younger and older half of the patients separately (VBM analysis for each CRPS group in contrast to their matched control subjects). Both CRPS sub-groups showed the same pattern of gray matter atrophy as in the whole group contrast (right AI and VMPFC extending into the NAc); however, only the younger group had a statistically significant result, with peak atrophy at right AI (Figure 2D). Gray matter density extracted from this cluster was significantly different between the groups ($p < 10^{-5}$), and showed a negative correlation with pain intensity scores ($R^2 = 0.52$ $p < 0.0001$; also significant non-parametrically) in this younger CRPS sub-grouping. The same brain region in the older grouping only showed a significant decrease between CRPS and healthy controls ($p < 0.02$).

White matter fractional anisotropy is decreased in the left cingulum bundle in CRPS

For each subject we calculated in each white matter voxel the FA value, which quantifies strength of directionality of the local tract structure. Whole-brain voxel-wise comparison, over the white matter skeleton, using permutation testing and stringent statistical thresholding, showed that CRPS patients have lower FA values in a cluster within the left callosal fiber tract, located just lateral to ACC (unpaired t-test, cluster $p = 0.03$; cluster size = 0.09 cm^3 ; with peak decreased FA at coordinates -16, 7, 33; t-value = 3.70, $p = 0.02$) (Figure 3A). The opposite contrast, searching for increased FA in CRPS, was empty. The possibility that the observed difference between patients and control was due to a difference in the amount of displacement applied during registration was ruled out (Figure S4B). Decreases in FA can be driven by various combinations of increases (λ_1) or decreases in the parallel and perpendicular diffusion components (λ_2 and λ_3). In the area showing a decrease in FA in CRPS, mean parallel diffusivity was significantly larger in healthy subjects (0.36 ± 0.05) compared to CRPS patients (0.35 ± 0.05), whereas mean perpendicular diffusivity was significantly less in healthy subjects (0.15 ± 0.03) compared to CRPS patients (0.17 ± 0.03) ($p < 0.01$). Therefore, water diffusion in this white matter cluster in the CRPS brain increased locally but decreased over the principal fiber direction.

White matter connectivity and branching indicate long-distance decreased connectivity and decreased and increased branchings in CRPS

To examine the properties of tracts passing through the regions with decreased FA or decreased gray matter density, we used probabilistic tractography to trace and quantify pathways from these clusters in both groups. To quantify tract properties we adapted the Sholl analysis (Sholl, 1953) to probabilistic tractography, where based on a fixed threshold of connectivity (Figure S6) the number of connections are counted as a function of Euclidean distance from the seed. We calculated, for each group and for each hemisphere, the mean number of connections as a function of distance from a given seed. Given that the Sholl analysis is closely related to the box counting method and can be used in quantifying fractal structures (Krauss et al., 1994; Mandelbrot, 1982), we also calculated cumulative sum of connections as a function of distance from the seed to measure the fractal dimension of branching patterns.

Connectivity and branching for a white matter seed—Thresholded group-averaged tract maps in CRPS and matched controls were determined using the white matter area with decreased FA in CRPS as the starting seed. This analysis identified callosal fibers, the cingulum bundle, parts of the superior longitudinal fasciculus, the cortico-pontine tract, and thalamic radiations. Additionally, in CRPS there seemed to be a prominent decrease in the probability of connections to the posterior cingulate area, a long-range connection, most likely part of the

cingulum bundle (Figure 3B). Using the adapted Sholl analysis, we observe that in the left hemisphere (ipsilateral to the seed), average number of connections at long distances (> 60 mm from seed), as well as total number of connections, were significantly lower in CRPS compared to healthy subjects ($p < 0.01$) (Figure 3C). The log-log graphs of the cumulative sum of connections as a function of distance (Figure 3C and Figure S7A) indicate a distance scaling range (S_d) within which connectivity follows a linear region, where the slope identifies fractal dimension (D_f) for the branching pattern of the tract. In the left hemisphere (ipsilateral to the seed), mean fractal dimension was significantly less in CRPS, whereas the scaling range was significantly longer. These findings indicate that the structure of this tract is disrupted even in the short distances, and the branching pattern is less space filling in CRPS. No significant differences were found in these measures in the right hemisphere (Figure 3C and Supplemental Table 2).

Connectivity and branching for gray matter seeds—Decreases in gray matter density can be due to loss of tissue from neurodegeneration (cell death) or volume shrinkage without cell death (Apkarian et al., 2004b; Apkarian and Scholz, 2006; Kuchinad et al., 2007). However, loss of gray matter density with concomitant loss of white matter connectivity would provide further evidence for the neurodegeneration hypothesis. We therefore studied white matter connectivity for the gray matter areas showing decreased density in CRPS. Performing probabilistic tractography, and using the portion of the right VMPFC exhibiting decreased gray matter density as the seed, we identified tracts in the callosal bundle, inferior fronto-occipital and longitudinal fasciculi, in addition to parts of the uncinate fasciculus, and fornix connections (Figure 4A). In CRPS, the long distance tracts (> 100 mm) ipsilateral to the seed showed reduced probability for connections, especially in the fronto-occipital and longitudinal fasciculi, resulting in reduced total number of connections. Contralateral connectivity showed increases at specific distances (around 80 mm and 120 mm from the seed) but no change in total connectivity (Figure 4B). Remarkably, for this seed branching pattern in the contralateral hemisphere was more space filling in CRPS (Figure S9B and Supplemental Table 2). We also investigated seed to gray matter targets for a number of brain regions (only ipsilateral connections were studied), and seed to other gray matter seeds in regions showing atrophy. In CRPS, connections from the VMPFC seed were higher to the whole insula and to seed AI, lower to the basal ganglion, and unchanged to the thalamus, primary somatosensory cortex, visual cortex, and to NAc seed (Figure 4C and Figure S8).

We performed the same type of analysis for the right AI region showing reduced gray matter density. Unlike the VMPFC seed, the AI seed had little contralateral connectivity (Figure 5A). Ipsilaterally, the most represented white matter bundles included the inferior fronto-occipital and longitudinal fasciculi, the uncinate fasciculus, and parts of the superior longitudinal fasciculus. In CRPS, the ipsilateral total number of connections was significantly less, although at around 100 mm from the seed there was a prominent increase in connectivity (Figure 5B). Moreover, the fractal dimension was significantly decreased in CRPS patients, implying reduced space filling (Figure S7C and Supplemental Table 2). Seed to gray matter target connectivity indicated decreased connections only to the basal ganglion and NAc seed (Figure 5C Figure S8).

Seed to seed connectivity—We performed seed to seed connectivity analyses between the right VMPFC, AI and NAc gray matter regions that showed reduced density in CRPS. In CRPS, connection counts from right AI to VMPFC were increased, while those from right NAc to AI were decreased. In addition, we found that the connection count from right VMPFC to NAc was significantly positively correlated with two separate anxiety scores in CRPS patients (Beck's Anxiety Index and Pain Anxiety Symptom Scale) (Figure S8).

Discussion

The main outcome of the current study is the observation that CRPS patients exhibit regional gray matter atrophy in a single cluster encompassing right VMPFC, AI and NAc, localized decreased white matter anisotropy, and changes in branching and connectivity of white matter tracts linked to these site-specific gray and white matter abnormalities. Unlike results from chronic back pain and fibromyalgia (Apkarian et al., 2004b; Kuchinad et al., 2007), whole-brain gray matter and ventricular size were similar between CRPS and control subjects. Aging effects on whole-brain gray matter volume was similar but smaller than that seen in fibromyalgia (Kuchinad et al., 2007), suggesting a smaller impact of the condition on whole-brain gray matter parameters. Notably, the relationship between brain white matter skeletal FA and brain gray matter volume seems completely disrupted in CRPS, implying reorganization of white matter tracks in a manner that no longer conforms to the relationship seen in healthy subjects. As this is a disruption at the whole-brain level, it entails either diffuse disruption of gray to white matter relationships or multiple distinct abnormalities with compensatory remodeling of the brain in CRPS.

Role of *right* anterior insula in CRPS symptoms

Regional gray matter density comparison indicated atrophy within a single cluster for the whole group of CRPS. The same brain region or portions of the same cluster exhibited atrophy even after subdividing the group by age or by laterality of CRPS pain. Hence the atrophy spanning AI, VMPFC, and NAc seems a robust result in CRPS and is right hemisphere dominant. Moreover, this atrophy was related to the two fundamental clinical characteristics of CRPS, duration and intensity, which impacted the density of this cluster above and beyond normal aging. When the cluster was subdivided into separate anatomical regions, the right AI correlated with duration of CRPS pain. The insula is the brain structure most often observed activated in acute pain tasks (Apkarian et al., 2005). In CRPS patients, bilateral AI activity correlates with ratings of touch-induced pain (allodynia), as well as to pin-prick hyperalgesia (Maihofner et al., 2005; Maihofner et al., 2006). Moreover, recent human brain imaging studies, consistent with the older literature regarding the role of the insula as a viscerosensory cortex (Craig, 2002; Saper, 2002), highlight the role of the *right* AI in the representation of autonomic and visceral responses (Critchley, 2005). Patients with pure autonomic failure due to peripheral disruption of autonomic responses exhibit reduced *right* AI activity (Critchley et al., 2001), and atrophy in *right* AI (Critchley et al., 2003a). In healthy subjects, neural activity in *right* AI predicts subjects' accuracy in heartbeat detection, while local gray matter volume, at coordinates closely approximating the center of the cluster we observed atrophied in our CRPS patients, correlates with subjective ratings of visceral awareness (Critchley et al., 2004). Furthermore, by comparing brain activity and autonomic responses in a fear conditioning task between healthy subjects and pure autonomic failure patients, Critchley and colleagues conclude that the *right* AI is involved in emotional representations, "wherein 'feelings' are the integration of both the mapping of internal arousal and conscious awareness of emotional stimuli" (Critchley et al., 2002). Given that CRPS patients are presumed to be in a constant negative emotional state and exhibit multiple signs of abnormal autonomic function, atrophy of *right* AI in CRPS corroborates the above studies and suggests that central anatomical abnormalities may explain fundamental symptoms of CRPS.

Role of VMPFC in CRPS in relation to emotional decision-making

Atrophy in the right VMPFC was correlated with the interaction of duration and intensity of CRPS pain, which functionally segregates the atrophy in this region from right AI and suggests a more global impact, or 'emotional load', of CRPS on the VMPFC. Atrophy within this region was our primary hypothesis as CRPS patients perform poorly on the emotional decision-making task (Apkarian et al., 2004a), which has been shown to critically depend on an intact

VMPFC (Bechara et al., 2000). In fact, even when CRPS pain is transiently reduced, performance on this task does not improve and CRPS patients do not show evidence of learning the task (Apkarian et al., 2004a). In contrast, chronic back pain patients who exhibit atrophy in the thalamus and dorsolateral prefrontal cortex (DLPFC) (Apkarian et al., 2004b), although also abnormal on this task, exhibit clear signs of learning and improved performance over time. Emotional decision-making critically depends on the ability to evaluate options in terms of potential reward or punishment; such decisions require proper capturing and evaluation of sensory cues, including bodily autonomic responses. It is thus not surprising that autonomic regulation and monitoring involve many of the same cortical regions implicated in emotional decision-making, especially ACC, VMPFC and AI. Therefore differential atrophy of gray matter and abnormal connectivity of associated white matter tracks involving ACC, VMPFC, and AI in CRPS, in contrast to atrophy of DLPFC in chronic back pain must underlie their differential responses on emotional decision-making, especially given the fact that CRPS is associated with autonomic abnormalities and chronic back pain is not.

Neurons within the VMPFC encode the emotional value of sensory stimuli (Kringelbach, 2005; Rolls, 2000). Moreover, patients with VMPFC lesions exhibit diminished emotional responses and social emotions (Anderson et al., 1999), as well as poorly regulated anger and frustration tolerance (Koenigs and Tranel, 2007). A recent study showed also abnormal utilitarian judgments on moral dilemmas that pit considerations of aggregate welfare against emotionally aversive behaviors (Koenigs et al., 2007). Parts of the region are activated during anticipation of pain (Porro et al., 2002), anticipation of placebo (Wager et al., 2004), when acute pain is enhanced (Lorenz et al., 2002), and especially when spontaneous pain of chronic back pain is high and sustained (Baliki et al., 2006; Baliki et al., 2008). Importantly, this region projects to the hypothalamus and brainstem areas that link autonomic bodily processes with emotional responses (Ongur and Price, 2000). It also projects to the periaqueductal gray thereby modulating spinal cord responses to nociceptive inputs (An et al., 1998). Hence the VMPFC region together with AI may be directly involved in determining characteristics of CRPS pain and associated autonomic abnormalities. We also demonstrated that the strength of white matter connectivity between VMPFC and NAc was related to the heightened anxiety generally seen in such patients. This is consistent with studies on mood and anxiety disorders emphasizing the role of hyperactivity in Brodmann area 25, part of VMPFC, in the pathophysiology of depression and its response to treatment (Ressler and Mayberg, 2007). Deep brain stimulation in the same white matter bundles we mapped here between NAc and VMPFC leads to decreased brain activity in VMPFC and remission of symptoms in treatment resistant depression (Mayberg et al., 2005).

Cingulum bundle decreased FA and its potential contribution to CRPS motor and cardiovascular abnormalities

Voxel based comparison of FA showed a single cluster with decreased anisotropy in the left callosal bundle, decreased parallel diffusivity and increased perpendicular diffusivity suggesting loss of axons and/or loss of myelination in CRPS; this can be interpreted as an injured white matter bundle (Beaulieu, 2002), although interpretation of changes in diffusion parameters is not straightforward and track geometry alterations may produce similar results. Connectivity from this cluster in CRPS was lower for long distances, and local branching patterns were less space filling. Both results are consistent and complimentary to the notion of loss of axons and/or injury. This regional white matter decrease in FA could not be related to clinical characteristics of CRPS, and did not connect to the gray matter regions showing atrophy in the opposite hemisphere. It therefore appears to be an independent brain injury observed in CRPS, unrelated to gray matter atrophy. Decreased FA in a region closely approximating the area observed here has been described in obsessive-compulsive disorder (An et al., 1998; Szeszko et al., 2005). The area of decreased FA in CRPS was located just lateral to the ACC,

and the tracts identified in the region included bilateral pathways between the ACC and supplementary motor area, interconnecting ACC with other portions of the cingulum, as well as to the thalamus. Therefore, the injured bundle seems to affect connectivity of ACC and SMA, a region repeatedly implicated in acute pain perception (Apkarian et al., 2005), especially the affective component (Rainville et al., 1997). The ACC is shown to be preferentially activated for touch-evoked pain in CRPS, a pain commonly observed in and around the traumatized limb, with fMRI activity correlating to the magnitude of the perceived pain (Maihofner et al., 2006). SMA/pre-SMA activity, on the other hand, correlates to the patients' motor impairments (Maihofner et al., 2007). Moreover, a recent study indicates that activity in ACC is related to modulation of heart rate, and patients with focal damage involving the ACC show abnormalities in cardiovascular responses (Critchley et al., 2003b). Abnormal cardiovascular responses have also been identified in adolescent CRPS patients (Meier et al., 2006). Thus the decreased anisotropy and associated decreased connectivity for the white matter just lateral to ACC and SMA observed here may contribute to both the perception of CRPS pain and associated motor and cardiovascular abnormalities.

Inter-relating gray matter atrophy and white matter reorganization

The decreased gray matter density in CRPS may be due to various neurobiological causes: atrophy secondary to excitotoxicity and/or exposure to inflammation-related agents, such as cytokines (Apkarian et al., 2004b; Apkarian and Scholz, 2006; Kuchinad et al., 2007), decreased cell size, synaptic pruning, decreased number of glia (with little or no neuronal death) (Schmidt-Wilcke et al., 2007), or genetic predisposition. Examining white matter properties for gray matter regions showing atrophy enabled us to exclude some of these mechanisms. From the VMPFC and AI gray matter seeds we observe that ipsilateral long distance and total connections decreased in CRPS, consistent with the atrophy hypothesis. Connectivity at specific distances either ipsilaterally or contralaterally, however, also indicated increased values. Moreover, the fractal dimension for nearby branchings was decreased from AI but increased from VMPFC. Similarly, seed to target connections were decreased to the basal ganglia from both seeds but increased from VMPFC to insula. Thus, in addition to atrophy, white matter properties also suggest rewiring with evidence for synaptic pruning and target specific rewiring. While the causal relationship between these changes and CRPS onset remains unclear, the correlations between brain atrophy and CRPS duration suggest that at least some of the gray matter changes are a consequence of living with CRPS.

Technical issues

Combining VBM gray matter morphometry with DTI white matter tractography provides a powerful approach to studying brain anatomical abnormalities in chronic pain. Even though both methods are validated and reproducible within and across subjects, the sensitivity and specificity of DTI remains less explored. As both approaches use whole-brain repeat measures corrected comparisons, they invariably only identify the most robust abnormalities. Approaches for analyzing DTI data continue to develop, with recent advances showing better sensitivity (Behrens et al., 2007). Thus it is quite likely that the single fiber based approach used here for probabilistic tractography missed some tracks, especially at the decreased FA area where the smaller cingulum and larger callosal pathways cross as a result we may have under estimated the contribution of the former.

The quantification methods developed here show that DTI-based probabilistic tractography can distinguish subtle differences in connectivity and branching pattern of studied tracts. The fractal dimension for seeds placed in distinct Brodmann areas indicated different branching properties. Therefore, the general rules underlying branching properties of DTI-based gray and white matter seeded tracts can be characterized, and may provide new metrics with which the human brain can be mapped. It should however be emphasized that the approach used here for

quantifying branching and connectivity changes remain rather speculative and requires validation by more direct anatomical tracing techniques, perhaps in animal models of chronic pain.

Pain intensity and duration were the primary CRPS characteristics that we tried to relate to gray and white matter properties. Anxiety, depression, medication use and age were secondarily examined to explore their relationships individually or as covariates. As most of these variables were skewed, we also tested relationships non-parametrically. The correlation coefficients were not corrected for multiple comparisons, yet the weaker relationships ($p > 0.005$) should be viewed as primarily indicative of trends.

Conclusions

We provide several lines of evidence indicating that the patient with CRPS has multiple pathological changes of the brain. We observe global disorganization of the relationship between gray and white matter in these subjects. Regional gray matter atrophy seems limited to brain regions that can be related to these patients' deficits in emotional decision-making and abnormal sympathetic outflow. Regional white matter anisotropy was observed in a bundle in the hemisphere contralateral to the gray matter atrophy, where long distance connections and branching patterns were reduced. The inter-relationship between gray matter atrophy and white matter connectivity provided evidence for both decreased long distance connectivity and regional increases and decreases in connectivity and branching patterns. These results suggest that the abnormal anatomy of the CRPS brain may underlie many of the autonomic, cognitive, and pain abnormalities seen in this pernicious syndrome.

Experimental Procedures

Subjects

The pool of subjects included 26 patients with CRPS and 28 healthy controls. CRPS patients were recruited from local clinics in Chicago, as well as a clinic in Toledo, Ohio. They were diagnosed according to the statistical modification of the IASP criteria for CRPS (Harden et al., 1999; Harden et al., 2007). The more specific criteria (the 'research' criteria) were used: e.g. all patients reported continuing pain "disproportionate to the inciting event" in addition to at least one symptom in each of the four symptom categories and signs in two of the four sign categories, for at least 3 months (range 3 months to 13.5 years). Clinical characteristics are summarized in Supplementary Table 1a and 1b. Patients were excluded if they reported other chronic painful conditions, systemic disease, history of head injury or coma, or psychiatric diseases. Depression is a common co-morbidity of CRPS (Bruehl and Carlson, 1992). Therefore, patients reporting more than mild to moderate depression, as defined by Beck's Depression Index (BDI > 19) were excluded (one CRPS patient had a BDI score of 28, all others' score was < 18). No cutoff threshold was used for anxiety. Healthy subjects were recruited from advertisements in local print media, and were matched for age and sex to the patients. Except for the CRPS signs and symptoms, the same inclusion and exclusion criteria were used in choosing healthy controls. The Northwestern University Institutional Review Board approved this study, and written informed consent was obtained from all participants.

Scanning

We used a 3T scanner (Siemens, Germany) to acquire both high resolution T1-images and diffusion tensor images (DTI) in a single session. MPRAGE type T1-anatomical images were acquired using the following parameters: voxel size $1 \times 1 \times 1$ mm; TR, 2500 ms; TE, 3.36 ms; flip angle = 9° ; in-plane matrix resolution, 256×256 ; slices, 160; field of view, 256 mm. DTI images were acquired using spin-echo echo-planar imaging (EPI) in two acquisitions 36 slices each, shifted in the z-direction to cover the whole-brain. DTI parameters were: voxel size 1.7

$\times 1.7 \times 2$ mm in 18 of the 21 CRPS patients and 16 of the control subjects respectively, and $2 \times 2 \times 2$ mm in the remaining 3 CRPS patients and 5 control subjects respectively; TR, 5000 ms; TE, 87 ms; flip angle, 90 degrees; in-plane matrix resolution, 128×128 ; field of view 220×220 mm; b_0 , 1000 s/mm²; diffusion was measured in 60 different non-collinear directions separated in time into 7 groups by no-diffusion weighted volumes for a total of 8 no-diffusion weighted volumes acquired for the purposes of registration and head motion correction.

Morphometry

Twenty-two CRPS patients (19 females, 3 males, mean age \pm s.e.m. = 40.7 ± 2.3 years old) and 22 age and sex matched healthy controls (19 females, 3 males, 40.5 ± 2.3 years old) from our subject pool were included in this analysis. The T1-anatomical brain images were used to calculate cortical gray matter volume, skull normalized to a standard brain (to compensate for body-mass variations), excluding the cerebellum and deep gray matter and brainstem. T1 images were also used to calculate skull-normalized lateral ventricular volumes, using an in house made mask for this purpose. These measures were derived by the cross-sectional version of SIENA, SIENAX, part of FSL 3.3 software (<http://www.fmrib.ox.ac.uk/fsl/>), which uses an automated brain extraction and tissue segmentation algorithm to yield estimates of volumes of interest (Smith et al., 2002; Smith et al., 2004).

Regional gray matter density was assessed with voxel-based morphometry (VBM) using the optimized method and non-parametric statistical contrasts (Ashburner and Friston, 2000; Good et al., 2001). The FSL 4.0 software was used for brain extraction (Smith et al., 2004) and segmentation (Zhang et al., 2001), and the IRTK tool for non-rigid transformation using spline-based deformation (Rueckert et al., 1999) to spatially register the native images. The protocol included the following steps: first, a left-right symmetric study specific gray matter template was built from 44 gray matter-segmented native images and their respective mirror images that were all affine-registered to a standard gray matter template (ICBM-152). The gray matter volume images were then non-linearly normalized onto this template. The optimized protocol introduces a compensation ('modulation') for the contraction/enlargement due to non-linear component of the transformation: each voxel of registered gray matter image was divided by the Jacobian of the warp field. Finally, in order to choose the best smoothing kernel, all 44 modulated, normalized gray matter volume images were smoothed with increasing size isotropic Gaussian kernels ($\sigma = 2.5, 3, 3.5, \text{ and } 4$ mm, corresponding to a 6, 7, 8, and 9.2 mm FWHM).

Regional changes in gray matter were assessed using permutation-based inference (Nichols and Holmes, 2002) to allow rigorous cluster-based comparisons of significance within the framework of the general linear model using a p -value < 0.05 . Group differences were tested against 5000 random permutations, which inherently accounts for multiple comparisons. Age and total intracranial volume were both used as variables of no-interest. Region of interest (ROI) analyses were performed on those areas showing significant group differences, by extracting VBM values and comparing between groups. To anatomically delineate the brain areas encompassed within the cluster showing significant group differences, we used conjunction analysis between the cluster and anatomic regions based on the macroscopic anatomical parcellation of the MNI MRI-single subject brain (Tzourio-Mazoyer et al., 2002). Thus, each ROI was composed of voxels significantly different between the groups and belonging to a given anatomical structure. Mean gray matter density over the ROIs was extracted and regressed against CRPS characteristics.

DTI analysis

Twenty-one CRPS patients (18 females, 3 males, 39.4 ± 2.4 years old) and 21 age and sex matched healthy controls (18 females, 3 males, 39.2 ± 2.4 years old) from our subject pool

were included in this analysis. We calculated fractional anisotropy (FA) for each voxel, which reflects the degree of diffusion anisotropy within a voxel (range 0-1, where large values indicate directional dependence of Brownian motion due to white matter tracts and smaller values indicate more isotropic diffusion and less coherence) (Beaulieu, 2002), FDT in FSL 3.3 was used (Smith et al., 2004). Correction for eddy-currents and head motion was done by means of affine registration on the first no-diffusion weighted volume of each subject. FA images were created by fitting the diffusion tensor to the raw diffusion data, after brain extraction using BET (Smith, 2002). Voxel-wise statistical analysis of FA data was carried out using tract-based spatial statistics (TBSS) part of FSL (Smith et al., 2006). All subjects' FA data (CRPS patients and matched healthy controls) were re-aligned into a common space, which was a healthy control subject's FA image, using the non-linear IRTK registration tool. The mean FA image was then created and thinned to create a mean FA skeleton representing the centers of all tracts common to the group. Each subject's aligned FA data was then projected back onto this skeleton. The significance of the comparison between CRPS patients and controls was determined using permutation testing ($n = 5000$ permutations, $p < 0.05$). An unpaired t-test model was used where age and voxel size were included as variables of no interest. For the area where CRPS patients showed a significant difference from control, we extracted individual average FA and compared it between the groups. We also calculated the mean skeletal brain FA, as a global index of diffusion in the white matter (Giorgio et al., 2007), by averaging FA values over each subject's white matter skeleton. This parameter was compared between groups and regressed against CRPS characteristics. We similarly calculated group maps of the primary diffusion directions (λ_1 : parallel diffusivity, $\lambda_2+\lambda_3/2$: perpendicular diffusivity to the principal diffusion direction). For the area where CRPS patients showed a significant FA difference, we tested whether the groups differed in the component diffusivities. We also calculated mean skeletal brain λ_1 , and mean skeletal brain $(\lambda_2+\lambda_3/2)$ by averaging values over each subject's white matter skeleton and compared between groups.

We performed probabilistic tractography using FDT (Behrens et al., 2003) by first running Markov-chain Monte Carlo sampling to build up distributions on the diffusion parameters at each voxel in the individual subject's space. Seeds of interest were defined in gray and white matter standard space (based on VBM and FA outcomes) and transformed into individual subject DTI space. From each seed voxel, 5000 samples were drawn to build the *a posteriori* distribution of the connectivity distribution. Average connectivity maps were generated in MNI space by transforming individual connectivity distributions. In each subject, we set a fixed threshold of 50 out of 5000 samples (see Figure S6) to determine the presence (1) or the absence (0) of a tract at each voxel. We then added the binary subjects' maps for healthy and CRPS subjects separately. In the resulting map a value of 21 indicated a voxel in which each subject from that group had a supra-threshold probability of connection from the seed. Connectivity-distance relationships were examined by performing a Sholl type analysis (Sholl, 1953) in each individual map, where number of connections were counted as a function of distance from the seed. These were then averaged and compared between groups. We also measured the cumulative number of connections as a function of distance, and used these measures to calculate a fractal dimension for the branching pattern of the connectivity. Cumulative connections as a function of distance (in log-log space) was used to determine a distance range (S_d) over which we could fit a straight line (least-square method was used to determine optimum distance range), the slope of the line identified the fractal dimension D_f . These parameters were compared between the two groups.

We quantified the probability of connections from gray matter seeds to specific targets in the ipsilateral right hemisphere. Target ROIs were derived from MNI MRI-single subject brain (Tzourio-Mazoyer et al., 2002) and included the right thalamus, basal ganglion, primary somatosensory cortex, and the visual cortex. In addition, gray matter seeds were used as targets

for other gray matter seeds. Seed to target connectivity counts were summed across voxels and compared between groups, using non-parametric tests.

Pain and mood characteristics

CRPS patients completed the short-form of the McGill pain questionnaire (Melzack, 1987) and the Washington Neuropathic Pain Scale (Galer and Jensen, 1997). Pain intensity was assessed on scan day with a visual analog scale (VAS) (0 = no pain, 100 = maximum imaginable pain). Duration of pain is reported in years, and drug consumption was calculated using the validated Medication Quantification Scale (MQS) (Harden et al., 2005), which reduces drugs used for different durations and doses to a single scalar. Anxiety and depression traits were determined by questionnaires (Beck and Steer, 1993a; Beck and Steer, 1993b; McCracken et al., 1992). Correlations between pain and mood characteristics are presented in Supplementary Table 3.

Supplementary Material

Refer to Web version on PubMed Central for supplementary material.

Acknowledgements

This work was supported by a grant from the National Institutes of Health (NS35115). We thank all patients and volunteers for their participation, Dr. Dante R. Chialvo for help in quantitative techniques and helpful suggestions regarding data analysis and interpretation, and Elle Parks for help with language.

Reference List

- Alexander AL, Lee JE, Lazar M, Field AS. Diffusion tensor imaging of the brain. *Neurotherapeutics* 2007;4:316–329. [PubMed: 17599699]
- An X, Bandler R, Ongur D, Price JL. Prefrontal cortical projections to longitudinal columns in the midbrain periaqueductal gray in macaque monkeys. *J Comp Neurol* 1998;401:455–479. [PubMed: 9826273]
- Anderson SW, Bechara A, Damasio H, Tranel D, Damasio AR. Impairment of social and moral behavior related to early damage in human prefrontal cortex. *Nat Neurosci* 1999;2:1032–1037. [PubMed: 10526345]
- Apkarian AV, Bushnell MC, Treede RD, Zubieta JK. Human brain mechanisms of pain perception and regulation in health and disease. *Eur J Pain* 2005;9:463–484. [PubMed: 15979027]
- Apkarian AV, Scholz J. Shared mechanisms between chronic pain and neurodegenerative disease. *Drug Discovery Today: Disease Mechanisms* 2006;3:319–326.
- Apkarian AV, Sosa Y, Krauss BR, Thomas PS, Fredrickson BE, Levy RE, Harden R, Chialvo DR. Chronic pain patients are impaired on an emotional decision-making task. *Pain* 2004a;108:129–136. [PubMed: 15109516]
- Apkarian AV, Sosa Y, Sonty S, Levy RE, Harden R, Parrish T, Gitelman D. Chronic back pain is associated with decreased prefrontal and thalamic gray matter density. *J Neurosci* 2004b;24:10410–10415. [PubMed: 15548656]
- Apkarian AV, Thomas PS, Krauss BR, Szeverenyi NM. Prefrontal cortical hyperactivity in patients with sympathetically mediated chronic pain. *Neurosci Lett* 2001;311:193–197. [PubMed: 11578827]
- Ashburner J, Friston KJ. Voxel-based morphometry--the methods. *Neuroimage* 2000;11:805–821. [PubMed: 10860804]
- Baliki MN, Chialvo DR, Geha PY, Levy RM, Harden RN, Parrish TB, Apkarian AV. Chronic pain and the emotional brain: specific brain activity associated with spontaneous fluctuations of intensity of chronic back pain. *J Neurosci* 2006;26:12165–12173. [PubMed: 17122041]
- Baliki MN, Geha PY, Apkarian AV, Chialvo DR. Beyond feeling: chronic pain hurts the brain, disrupting the default-mode network dynamics. *J Neurosci* 2008;28:1398–1403. [PubMed: 18256259]

- Beaulieu C. The basis of anisotropic water diffusion in the nervous system - a technical review. *NMR Biomed* 2002;15:435–455. [PubMed: 12489094]
- Bechara A, Damasio AR, Damasio H, Anderson SW. Insensitivity to future consequences following damage to human prefrontal cortex. *Cognition* 1994;50:7–15. [PubMed: 8039375]
- Bechara A, Damasio H, Damasio AR. Emotion, decision making and the orbitofrontal cortex. *Cereb Cortex* 2000;10:295–307. [PubMed: 10731224]
- Beck, A.; Steer, R. Beck Depression Inventory. San Antonio: Psychological Corporation; 1993a.
- Beck, A.; Steer, R. Manual for the Beck Anxiety Inventory. San Antonio: Psychological Corporation; 1993b.
- Behrens TE, Berg HJ, Jbabdi S, Rushworth MF, Woolrich MW. Probabilistic diffusion tractography with multiple fibre orientations: What can we gain? *Neuroimage* 2007;34:144–155. [PubMed: 17070705]
- Behrens TE, Woolrich MW, Jenkinson M, Johansen-Berg H, Nunes RG, Clare S, Matthews PM, Brady JM, Smith SM. Characterization and propagation of uncertainty in diffusion-weighted MR imaging. *Magn Reson Med* 2003;50:1077–1088. [PubMed: 14587019]
- Birklein F, Schmelz M, Schifter S, Weber M. The important role of neuropeptides in complex regional pain syndrome. *Neurology* 2001;57:2179–2184. [PubMed: 11756594]
- Bruehl S, Carlson CR. Predisposing psychological factors in the development of reflex sympathetic dystrophy. A review of the empirical evidence. *Clin J Pain* 1992;8:287–299. [PubMed: 1493340]
- Craig AD. How do you feel? Interoception: the sense of the physiological condition of the body. *Nat Rev Neurosci* 2002;3:655–666. [PubMed: 12154366]
- Critchley HD. Neural mechanisms of autonomic, affective, and cognitive integration. *J Comp Neurol* 2005;493:154–166. [PubMed: 16254997]
- Critchley HD, Good CD, Ashburner J, Frackowiak RS, Mathias CJ, Dolan RJ. Changes in cerebral morphology consequent to peripheral autonomic denervation. *Neuroimage* 2003a;18:908–916. [PubMed: 12725766]
- Critchley HD, Mathias CJ, Dolan RJ. Neuroanatomical basis for first- and second-order representations of bodily states. *Nat Neurosci* 2001;4:207–212. [PubMed: 11175883]
- Critchley HD, Mathias CJ, Dolan RJ. Fear conditioning in humans: the influence of awareness and autonomic arousal on functional neuroanatomy. *Neuron* 2002;33:653–663. [PubMed: 11856537]
- Critchley HD, Mathias CJ, Josephs O, O'Doherty J, Zanini S, Dewar BK, Cipolotti L, Shallice T, Dolan RJ. Human cingulate cortex and autonomic control: converging neuroimaging and clinical evidence. *Brain* 2003b;126:2139–2152. [PubMed: 12821513]
- Critchley HD, Wiens S, Rotshtein P, Ohman A, Dolan RJ. Neural systems supporting interoceptive awareness. *Nat Neurosci* 2004;7:189–195. [PubMed: 14730305]
- Galer BS, Jensen MP. Development and preliminary validation of a pain measure specific to neuropathic pain: the Neuropathic Pain Scale. *Neurology* 1997;48:332–338. [PubMed: 9040716]
- Gieteling EW, van Rijn MA, de Jong BM, Hoogduin JM, Renken R, van Hilten JJ, Leenders KL. Cerebral activation during motor imagery in complex regional pain syndrome type 1 with dystonia. *Pain* 2008;134:302–309. [PubMed: 17561345]
- Giorgio A, Watkins KE, Douaud G, James AC, James S, De Stefano N, Matthews PM, Smith SM, Johansen-Berg H. Changes in white matter microstructure during adolescence. *Neuroimage*. 2007
- Good CD, Johnsrude IS, Ashburner J, Henson RN, Friston KJ, Frackowiak RS. A voxel-based morphometric study of ageing in 465 normal adult human brains. *Neuroimage* 2001;14:21–36. [PubMed: 11525331]
- Harden, RN.; Baron, R.; Janig, W. Complex regional pain syndrome. Seattle: IASP Press; 2001.
- Harden RN, Bruehl S, Galer BS, Saltz S, Bertram M, Backonja M, Gayles R, Rudin N, Bhugra MK, Stanton-Hicks M. Complex regional pain syndrome: are the IASP diagnostic criteria valid and sufficiently comprehensive? *Pain* 1999;83:211–219. [PubMed: 10534592]
- Harden RN, Bruehl S, Stanton-Hicks M, Wilson PR. Proposed new diagnostic criteria for complex regional pain syndrome. *Pain Med* 2007;8:326–331. [PubMed: 17610454]
- Harden RN, Weinland SR, Remble TA, Houle TT, Colio S, Steedman S, Kee WG. Medication Quantification Scale Version III: update in medication classes and revised detriment weights by survey of American Pain Society Physicians. *J Pain* 2005;6:364–371. [PubMed: 15943958]

- Janig W, Baron R. Complex regional pain syndrome is a disease of the central nervous system. *Clin Auton Res* 2002;12:150–164. [PubMed: 12269546]
- Janig W, Baron R. Complex regional pain syndrome: mystery explained? *Lancet Neurol* 2003;2:687–697. [PubMed: 14572737]
- Kochunov P, Thompson PM, Lancaster JL, Bartzokis G, Smith S, Coyle T, Royall DR, Laird A, Fox PT. Relationship between white matter fractional anisotropy and other indices of cerebral health in normal aging: tract-based spatial statistics study of aging. *Neuroimage* 2007;35:478–487. [PubMed: 17292629]
- Koenigs M, Tranel D. Irrational economic decision-making after ventromedial prefrontal damage: evidence from the Ultimatum Game. *J Neurosci* 2007;27:951–956. [PubMed: 17251437]
- Koenigs M, Young L, Adolphs R, Tranel D, Cushman F, Hauser M, Damasio A. Damage to the prefrontal cortex increases utilitarian moral judgements. *Nature* 2007;446:908–911. [PubMed: 17377536]
- Krauss BR, Serog BJ, Chialvo DR, Apkarian AV. Dendritic Complexity and the Evolution of cerebellar Purkinje Cells. *Fractals* 1994;2:95–102.
- Kringelbach ML. The human orbitofrontal cortex: linking reward to hedonic experience. *Nat Rev Neurosci* 2005;6:691–702. [PubMed: 16136173]
- Kuchinad A, Schweinhardt P, Seminowicz DA, Wood PB, Chizh BA, Bushnell MC. Accelerated brain gray matter loss in fibromyalgia patients: premature aging of the brain? *J Neurosci* 2007;27:4004–4007. [PubMed: 17428976]
- Lorenz J, Cross DJ, Minoshima S, Morrow TJ, Paulson PE, Casey KL. A unique representation of heat allodynia in the human brain. *Neuron* 2002;35:383–393. [PubMed: 12160755]
- Maihofner C, Baron R, DeCol R, Binder A, Birklein F, Deuschl G, Handwerker HO, Schattschneider J. The motor system shows adaptive changes in complex regional pain syndrome. *Brain* 2007;130:2671–2687. [PubMed: 17575278]
- Maihofner C, DeCol R. Decreased perceptual learning ability in complex regional pain syndrome. *Eur J Pain* 2007;11:903–909. [PubMed: 17451979]
- Maihofner C, Forster C, Birklein F, Neundorfer B, Handwerker HO. Brain processing during mechanical hyperalgesia in complex regional pain syndrome: a functional MRI study. *Pain* 2005;114:93–103. [PubMed: 15733635]
- Maihofner C, Handwerker HO, Birklein F. Functional imaging of allodynia in complex regional pain syndrome. *Neurology* 2006;66:711–717. [PubMed: 16534108]
- Maihofner C, Handwerker HO, Neundorfer B, Birklein F. Patterns of cortical reorganization in complex regional pain syndrome. *Neurology* 2003;61:1707–1715. [PubMed: 14694034]
- Mandelbrot BB. *The fractal geometry of nature*. 1982
- Mayberg HS, Lozano AM, Voon V, McNeely HE, Seminowicz D, Hamani C, Schwalb JM, Kennedy SH. Deep brain stimulation for treatment-resistant depression. *Neuron* 2005;45:651–660. [PubMed: 15748841]
- McCracken LM, Zayfert C, Gross RT. The Pain Anxiety Symptoms Scale: development and validation of a scale to measure fear of pain. *Pain* 1992;50:67–73. [PubMed: 1513605]
- Meier PM, Alexander ME, Sethna NF, De Jong-De Vos Van Steenwijk CC, Zurakowski D, Berde CB. Complex regional pain syndromes in children and adolescents: regional and systemic signs and symptoms and hemodynamic response to tilt table testing. *Clin J Pain* 2006;22:399–406. [PubMed: 16691095]
- Melzack R. The short-form McGill Pain Questionnaire. *Pain* 1987;30:191–197. [PubMed: 3670870]
- Nichols TE, Holmes AP. Nonparametric permutation tests for functional neuroimaging: a primer with examples. *Hum Brain Mapp* 2002;15:1–25. [PubMed: 11747097]
- Ochoa JL. Reflex sympathetic dystrophy: a disease of medical understanding. *Clin J Pain* 1992;8:363–366. [PubMed: 1493348]
- Ongur D, Price JL. The organization of networks within the orbital and medial prefrontal cortex of rats, monkeys and humans. *Cereb Cortex* 2000;10:206–219. [PubMed: 10731217]
- Pleger B, Ragert P, Schwenkreis P, Forster AF, Wilimzig C, Dinse H, Nicolas V, Maier C, Tegenthoff M. Patterns of cortical reorganization parallel impaired tactile discrimination and pain intensity in complex regional pain syndrome. *Neuroimage* 2006;32:503–510. [PubMed: 16753306]

- Porro CA, Baraldi P, Pagnoni G, Serafini M, Facchin P, Maieron M, Nichelli P. Does anticipation of pain affect cortical nociceptive systems? *J Neurosci* 2002;22:3206–3214. [PubMed: 11943821]
- Rainville P, Duncan GH, Price DD, Carrier B, Bushnell MC. Pain affect encoded in human anterior cingulate but not somatosensory cortex. *Science* 1997;277:968–971. [PubMed: 9252330]
- Resnick SM, Pham DL, Kraut MA, Zonderman AB, Davatzikos C. Longitudinal magnetic resonance imaging studies of older adults: a shrinking brain. *J Neurosci* 2003;23:3295–3301. [PubMed: 12716936]
- Ressler KJ, Mayberg HS. Targeting abnormal neural circuits in mood and anxiety disorders: from the laboratory to the clinic. *Nat Neurosci* 2007;10:1116–1124. [PubMed: 17726478]
- Rolls ET. The orbitofrontal cortex and reward. *Cereb Cortex* 2000;10:284–294. [PubMed: 10731223]
- Rueckert D, Sonoda LI, Hayes C, Hill DL, Leach MO, Hawkes DJ. Nonrigid registration using free-form deformations: application to breast MR images. *IEEE Trans Med Imaging* 1999;18:712–721. [PubMed: 10534053]
- Saper CB. The central autonomic nervous system: conscious visceral perception and autonomic pattern generation. *Annu Rev Neurosci* 2002;25:433–469. [PubMed: 12052916]
- Schmidt-Wilcke T, Leinisch E, Ganssbauer S, Draganski B, Bogdahn U, Altmepfenner J, May A. Affective components and intensity of pain correlate with structural differences in gray matter in chronic back pain patients. *Pain*. 2006
- Schmidt-Wilcke T, Leinisch E, Straube A, Kampfe N, Draganski B, Diener HC, Bogdahn U, May A. Gray matter decrease in patients with chronic tension type headache. *Neurology* 2005;65:1483–1486. [PubMed: 16275843]
- Schmidt-Wilcke T, Lueding R, Weigand T, Jurgens T, Schuierer G, Leinisch E, Bogdahn U. Striatal grey matter increase in patients suffering from fibromyalgia—a voxel-based morphometry study. *Pain* 2007;132:S109–S116. [PubMed: 17587497]
- Sholl DA. Dendritic organization in the neurons of the visual and motor cortices of the cat. *J Anat* 1953;87:387–406. [PubMed: 13117757]
- Smith SM. Fast robust automated brain extraction. *Hum Brain Mapp* 2002;17:143–155. [PubMed: 12391568]
- Smith SM, Jenkinson M, Johansen-Berg H, Rueckert D, Nichols TE, Mackay CE, Watkins KE, Ciccarelli O, Cader MZ, Matthews PM, Behrens TE. Tract-based spatial statistics: voxelwise analysis of multi-subject diffusion data. *Neuroimage* 2006;31:1487–1505. [PubMed: 16624579]
- Smith SM, Jenkinson M, Woolrich MW, Beckmann CF, Behrens TE, Johansen-Berg H, Bannister P, De Luca CJ, Drobnjak I, Flitney DE, Nianzy R, Saunders J, Vickers J, Zhang Y, De Stefano N, Brady JM, Matthews PM. Advances in functional and structural MR image analysis and implementation as FSL. *Neuroimage* 2004;23(S1):208–219.
- Smith SM, Zhang Y, Jenkinson M, Chen J, Matthews PM, Federico A, De Stefano N. Accurate, robust, and automated longitudinal and cross-sectional brain change analysis. *Neuroimage* 2002;17:479–489. [PubMed: 12482100]
- Stanton-Hicks M, Janig W, Hassenbusch S, Haddox JD, Boas R, Wilson P. Reflex sympathetic dystrophy: changing concepts and taxonomy. *Pain* 1995;63:127–133. [PubMed: 8577483]
- Szeszko PR, Ardekani BA, Ashtari M, Malhotra AK, Robinson DG, Bilder RM, Lim KO. White matter abnormalities in obsessive-compulsive disorder: a diffusion tensor imaging study. *Arch Gen Psychiatry* 2005;62:782–790. [PubMed: 15997020]
- Tzourio-Mazoyer N, Landeau B, Papathanassiou D, Crivello F, Etard O, Delcroix N, Mazoyer B, Joliot M. Automated anatomical labeling of activations in SPM using a macroscopic anatomical parcellation of the MNI MRI single-subject brain. *Neuroimage* 2002;15:273–289. [PubMed: 11771995]
- Valfre W, Rainero I, Bergui M, Pinessi L. Voxel-based morphometry reveals gray matter abnormalities in migraine. *Headache* 2008;48:109–117. [PubMed: 18184293]
- Veldman PH, Reynen HM, Arntz IE, Goris RJ. Signs and symptoms of reflex sympathetic dystrophy: prospective study of 829 patients. *Lancet* 1993;342:1012–1016. [PubMed: 8105263]
- Wager TD, Rilling JK, Smith EE, Sokolik A, Casey KL, Davidson RJ, Kosslyn SM, Rose RM, Cohen JD. Placebo-induced changes in FMRI in the anticipation and experience of pain. *Science* 2004;303:1162–1167. [PubMed: 14976306]

Zhang Y, Brady M, Smith S. Segmentation of brain MR images through a hidden Markov random field model and the expectation-maximization algorithm. *IEEE Trans Med Imaging* 2001;20:45–57. [PubMed: 11293691]

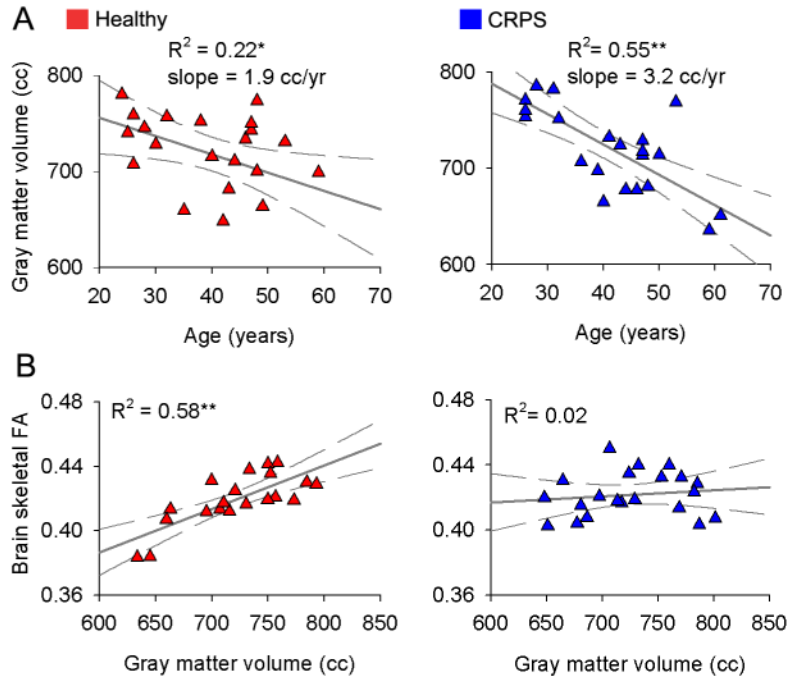


Figure 1. Whole-brain cortical gray volume and white matter anisotropy show distinct properties in CRPS as compared to matched healthy controls

(A) Skull normalized, neocortical gray matter volume in healthy (left) and CRPS patients (right) shown as a function of age.

(B) Whole-brain fractional anisotropy (mean FA calculated over individual subjects' white matter skeleton), a global measure of water diffusion over white matter tracks, in relation to whole-brain neocortical gray matter volume. The significant correlation between the two measures in healthy subjects is absent in CRPS.

* $p < 0.05$; ** $p < 0.01$.

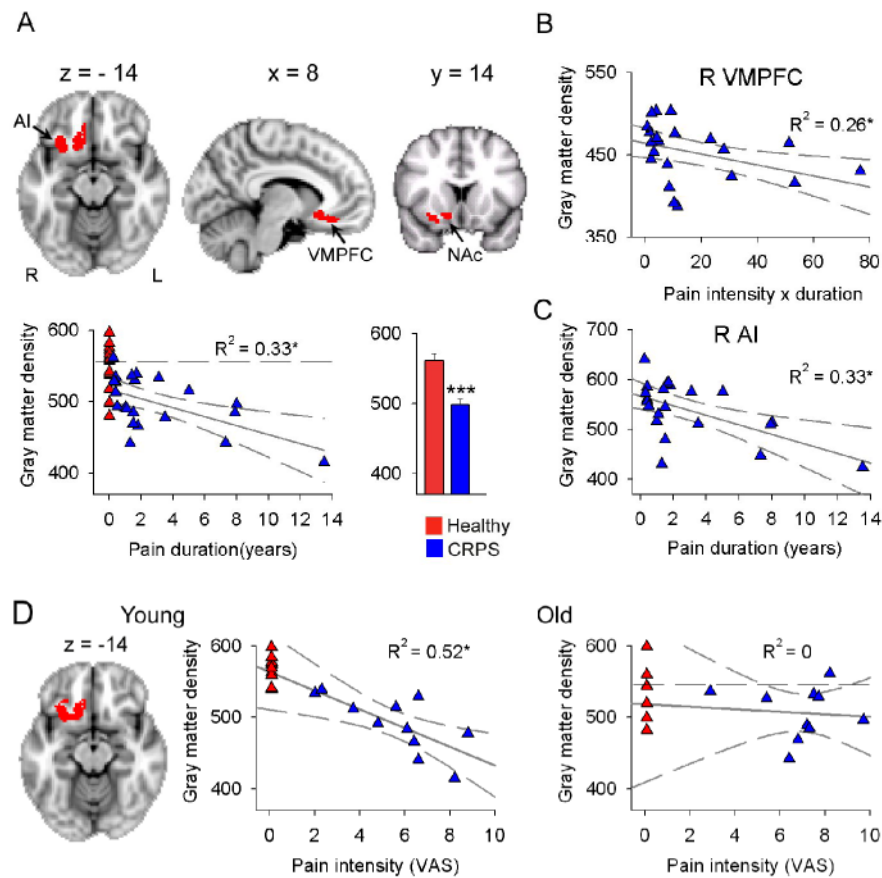


Figure 2. Brain regional gray matter density is decreased in CRPS, most prominently in the younger patients, and related to pain characteristics

(A) Voxel-based morphometry (VBM) comparison between CRPS and matched healthy control subjects indicates decreased density within a single cluster in the right hemisphere (red), spanning the ventromedial prefrontal cortex (VMPFC), anterior insula (AI), and nucleus accumbens (arrows) ($n = 22$ per group; $p < 0.05$ corrected). The scatter plot shows that this decreased gray matter density is negatively correlated to the number of years the patients have been living with CRPS. Individual control healthy subjects are shown at pain duration = 0. The histogram depicts mean (\pm SEMs) gray matter density within the cluster in both groups.

(B, C) Subdividing the cluster to its anatomic components, right VMPFC and right AI, shows that each region differentially related to CRPS pain characteristics: right VMPFC gray matter density negatively correlated to the interaction between pain intensity and pain duration (b); while right AI gray matter density only correlated to pain duration (c). (D) Subdividing the groups into young and old, and performing VBM contrast between CRPS and healthy controls for each sub-grouping shows that decreased gray matter density in young CRPS patients was localized to the same cluster as in the whole population. In the young subjects ($n = 11$ per group), a statistically significant decrease in gray matter density was observed (cluster p -value = 0.012; cluster size = 4.5 cm^3) with peak atrophy at right AI [coordinates, 28, 18, -12; t -value = 5.18, $p = 0.02$]. Gray matter density extracted from this cluster was significantly different between the groups ($p < 10^{-5}$), and showed a negative correlation with pain intensity scores (visual analog scale, 0-10). Whole-brain VBM contrast in the older sub-grouping was not significant. However, gray matter density extracted from the cluster derived from the young was significantly decreased ($p < 0.02$) but not correlated to pain intensity in the older CRPS

group. Individual control healthy subjects are shown at pain intensity = 0, and their mean gray matter density is indicated by a dashed lines.

* $p < 0.05$; *** $p < 10^{-5}$. R = right.

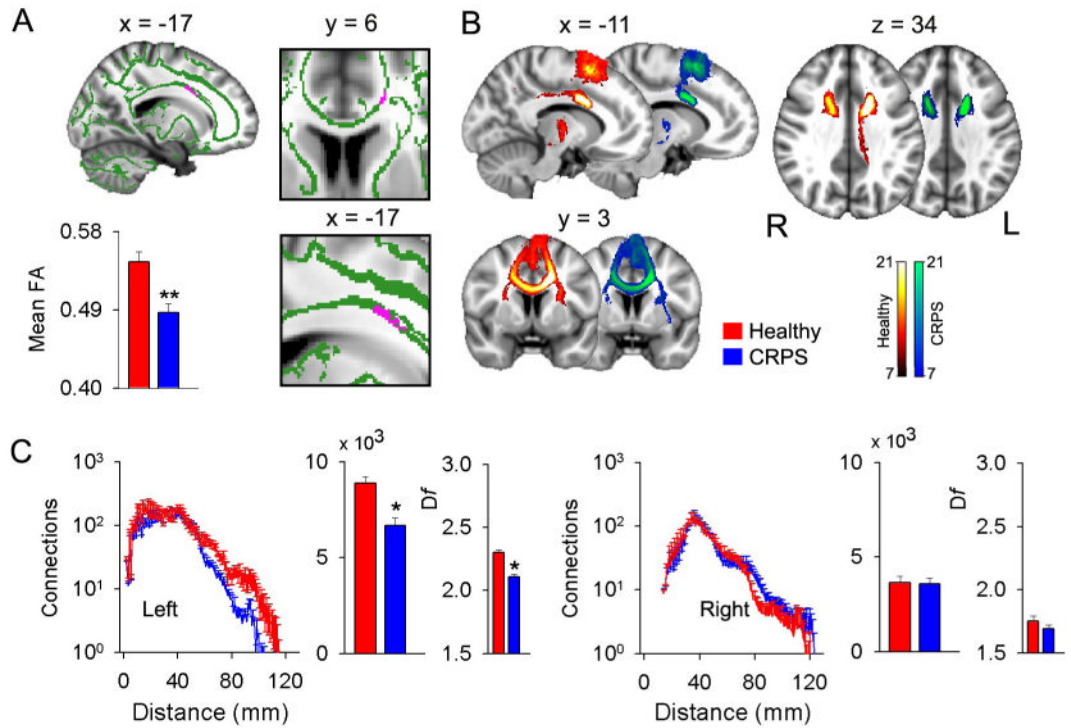


Figure 3. Decreased regional anisotropy and connectivity in CRPS as compared to matched healthy controls

(A) Contrasting FA (tested over the entire white matter skeleton, green) between CRPS and matched controls ($n = 21$ per group) indicates decreased FA in CRPS, localized to a portion of the left callosal fibers (purple, shown in different orientations and magnifications; $p < 0.05$ corrected). The histogram depicts mean FA (\pm SEMs) for the two groups, for the white matter region showing decreased FA.

(B) Population maps of results of probabilistic tractography when the white matter region showing decreased FA was used as the seed. Each color scale represents the population probability of a voxel belonging to the pathway tracked from the seed; voxels present in 33% (7/21, an arbitrary threshold used only for visualizing connectivity differences) of the population are shown. The tract traversing posteriorly in the healthy subjects belongs to the cingulum bundle and seems diminished in the CRPS patients.

(C) Quantitative differences in probabilistic connections and branching pattern for the pathway tracked from the seed (purple in a) are shown separately for left and right hemispheres. Group averaged number of connections (\pm SEMs) as a function of Euclidean distance shows that long distance connections in CRPS are only less in the hemisphere ipsilateral to the seed (left). First histogram shows total number of connections from the seed, and second histogram (thinner bars) the fractal dimension D_f of branching of connections (mean \pm SEMs). Both measures were significantly decreased in CRPS, again only in the hemisphere ipsilateral to the seed.

* $p < 0.05$ ** $p < 0.01$. R = right; L = left.

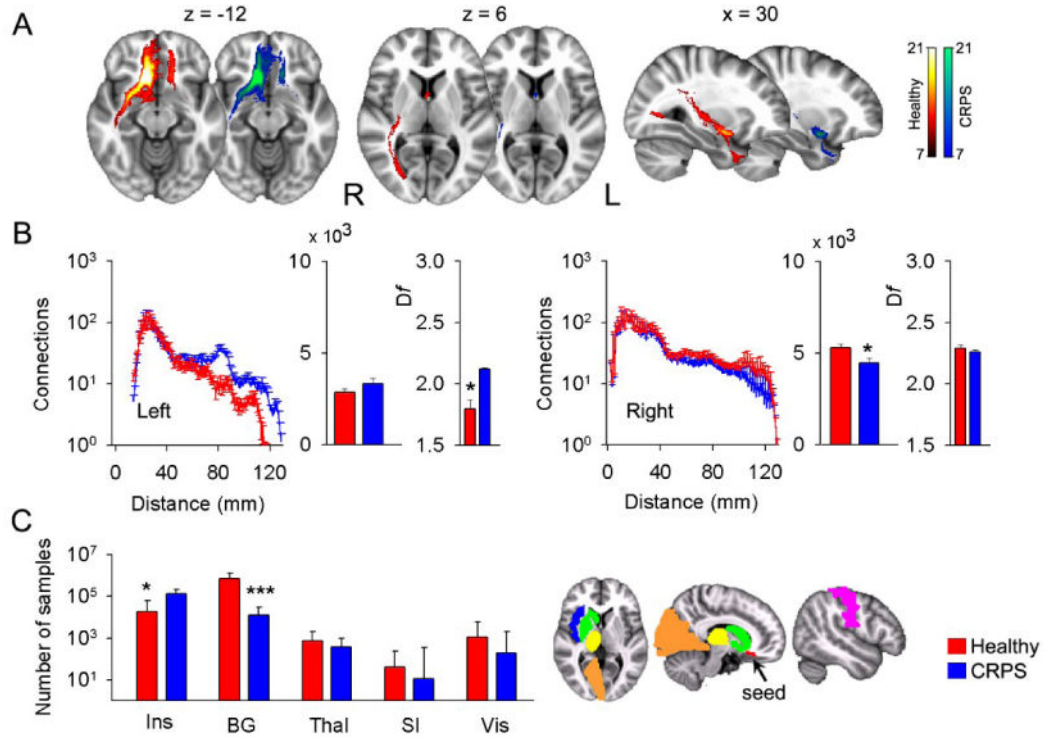


Figure 4. Gray matter decreased density in the right VMPFC is associated with reorganization of white matter connections in CRPS

Probabilistic maps of white matter tracts (A), connections as a function of distance, total connections and fractal dimension (histograms are mean ± SEMs) (B), and individual target connectivity (C) are depicted, when the portion of right VMPFC exhibiting decreased gray matter density is used as the seed.

(A & B) Ipsilateral connectivity is reduced mainly at long distances, while some regional connectivity and fractal dimension are increased contralaterally.

(C) In CRPS, target connectivity (examined only ipsilateral to the seed) is significantly higher to the insula (Ins) and lower to the basal ganglion (BG), but unchanged to the thalamus (Thal), primary somatosensory cortex (SI) and visual cortex (Vis) (medians and quartiles are shown). The colored brain masks illustrate the seed and targets used in connectivity calculations.

* $p < 0.05$; *** $p < 10^{-5}$.

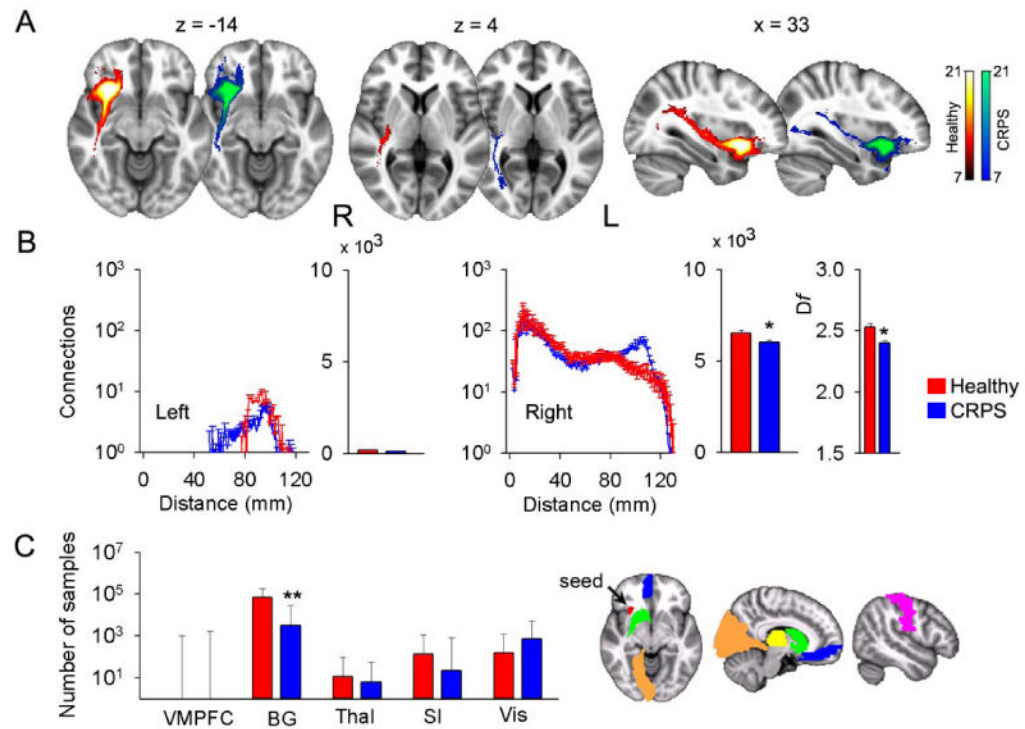


Figure 5. Decreased gray matter density in the right anterior insula is associated with reorganization of white matter connections in CRPS

Probabilistic maps of white matter tracts (A), connections as a function of distance, total connections, and fractal dimension (histograms are mean \pm SEMs) (B), and individual target connectivity (C) are depicted, when the portion of right insula exhibiting decreased gray matter density is used as a seed.

(A & B) Total ipsilateral connectivity and fractal dimension are reduced in CRPS, although there are also increased connections at specific distances. Contralateral connectivity is minimal from this seed.

(C) In CRPS, target connectivity is only reduced to the basal ganglia (medians and quartiles are shown).

* $p < 0.05$; ** $p < 10^{-3}$.